Low temperature heat source for power generation: Exhaustive analysis of a carbon dioxide transcritical power cycle.

Fredy Vélez[1], José Segovia[2], Farid Chejne[3], Gregorio Antolín[1], Ana Quijano[1], M. Carmen Martín[2]

(1) CARTIF Centro Tecnológico, División Químico-Alimentaria. Parque Tecnológico de Boecillo, Parcela 205. 47151 Valladolid, España .

(2) Grupo de Investigación TERMOCAL, Universidad de Valladolid, Paseo del cauce s/n, Valladolid, España.

(3) Grupo de Termodinámica Aplicada y Energías Alternativas TAYEA, Escuela de Procesos y Energía, Universidad Nacional de Colombia, Carr. 80 No. 65–223, Facultad de Minas, Medellín, Antioquia, Colombia.

Abstract.

The main results of a theoretical work on the use of a low temperature heat source for power generation through a carbon dioxide transcritical power cycle are reported in this paper. The procedure for analyzing the behaviour of the proposed cycle consisted in modifying the input pressure to the turbine from 66 bar, maintained constant each evaluated temperature (60 ºC, 90 ºC, 120 ºC and 150 ºC) until the net work was approximately zero. As a result, the maximum exergy efficiency was 50%, while the energy efficiencies obtained were 9.8%, 7.3%, 4.9% and 2.4% and the net specific work was 18.2 kJ/kg, 12.8 kJ/kg, 7.8 kJ/kg and 3.5 kJ/kg, respectively. Furthermore, the effect of the addition of an internal heat exchanger, which obviously supposed an increase in the efficiency, was analyzed. The analysis of the proposed system shows the viability of implementing this type of process as an energy alternative and/or strengthener of non-conventional energy sources in non-provided zones, or for increasing the energy efficiency in the industry.

Key words: Carbon dioxide; energy efficiency; exergy efficiency; power generation; waste heat.

Introduction.

At the present time, efforts must be focused on the energy supply successfully fulfilling the challenges of the modern world. The volatility of oil prices, global warming, the ozone layer depletion, the economic crisis, among others, are problems that require a joint effort with the aim of developing such renewable energies as solar, eolic, biomass, and geothermal, as well as the use of residual heat and/or at low enthalpy, thus achieving an efficient and rational use of energy [1].

Since conventional steam power cycles cannot give a better performance to recover low grade waste heat [2-5], it is necessary to analyze other types of processes, such as the organic Rankine cycle (ORC), whose most important feature is the availability of using different low temperature heat sources for power generation, as has been proposed by [6-12], among many other authors The researches realized have analyzed the performance and the use of ORC in different applications. In [4] was analyzed the efficiency of the ORC with waste heat of processes as well a regenerative ORC appears to be a choice system for converting low-grade waste heat to power from the analysis and optimization parametric done in [13]. In [11] it was analized how the waste heat from a conventional geothermal steam power plant can be efficiently utilized to generate electricity by installing a bottoming ORC. Other cycles ORC in bottoming cycles with internal combustion engine are shown in [9], whereas in [8] was designed and built a prototype low-temperature organic Rankine cycle system for reverse osmosis desalination.

However, the so-called pinching problem, due to the constant evaporation temperature of the organic substance, can occur in the ORC's counter current heat exchanger evaporator [14-15]. This is not suitable for sensible heat sources such as waste heat and therefore, some authors propose the same cycle, but with fluids working in supercritical conditions [14,16,17] and/or fluid mixtures [15] to achieve a variable temperature when heat is added to the working fluid for a better fit with the heat source. This phenomenon is known as

temperature ‘‘glide’’: different values of temperature at a given pressure. These processes are illustrated in Fig. 1.

From the viewpoint of protecting the ozone layer and preventing global warming, there is now a strong demand for technology based on ecologically safe “natural” working fluids, i.e. fluids like water, air, noble gases, hydrocarbons, ammonia and carbon dioxide [18]. Carbon dioxide (CO_2) as a natural refrigerant has attracted ever more interest in refrigeration applications. It is non-toxic, environment-friendly with an Ozone Depletion Potential (ODP) of zero [19] and a Global Warming Potential (GWP) of 1 over 100 years [20]. But it also has many advantages as a working fluid for power cycles, e.g. the moderate value of its critical pressure (73.8 bar), relative inertness (for the temperature range of interest), sufficient knowledge of its thermodynamic properties, being inexpensive, non-explosive and abundant in nature [6]. Furthermore, it may have a great potential to improve energy conversion in a more efficient way while greatly reducing the global discharge of CO_2 in the world by using waste heats from industrial processes and exhausted gases from combustion processes as the energy source of the system, increasing the electric energy produced with the same quantity of fuel but also employing renewable energy sources of low temperature such as the geothermal, solar, etc. It is also a manner of capturing CO_2 when it is utilized as working fluid, although this effect has rather minor importance because the environmental characteristics of this fluid can offer more important benefits.

Due to CO_2’s low critical temperature (31.1 ºC), the CO_2 power cycle in the current study will be a thermodynamic cycle where the working fluid goes through both subcritical and supercritical states, “a transcritical cycle”. However, the research and information available for the power cycle with CO_2 as working fluid in low temperature heat source for power generation is limited. In the last few years, the transcritical cycle with carbon dioxide has been studied with solar energy as the heat source at a temperature near 200 ºC in steady state [21], and an annual dynamic performance is simulated in [16]. A small-scale

prototype has been built and started up [18]. Its feasibility and efficiency has been shown to be between 8.78–9.45% [22]. The carbon dioxide transcritical power cycle (CDTPC) showed slightly higher power output than the ORC with an R123 as working fluid, according to the comparative study carried out in [6]. Finally, a methodology is presented in [14] and applied for the study of a CO_2 transcritical cycle supplied by a steady stream of low temperature process gases. These results have been calculated for fixed temperature and mass flow rate of the heat source, fixed maximum and minimum temperatures in the cycle and fixed sink temperature by varying the high pressure of the cycle and its net power output. Some of the researchers of [14] developed the study of the influence of the input temperature in the turbine (80 ºC – 99 ºC) on the total performance of the simple cycle, maintaining the same suppositions of the mentioned research, whose results are shown in [23].

The works on the transcritical power cycle with CO_2 [6,14,18,21-24] were carried out with water at a condensation temperature below 10 ºC, which increases the system's performance considerably, due to the higher pressure drop related to the higher value pressure of discharge that can be produced. In view of what has been stated, a lack of analysis has been detected on the influence of the input temperature in the turbine (60 ºC – 150 ºC) and therefore, the influence of the energy source on the performance and on the net specific work in a simple system and in a system with an internal heat exchanger (IHX). In this paper a water condensation temperature at 15 ºC is considered, which will allow these systems to be developed in a huge number of regions.

Main novelty aspects provided in the present paper are based in the scarce of information and researches leading to show the influence that have the input temperature and pressure to the turbine (and therefore of the energy source), as well as the including of an IHX for the power cycle with CO_2 as working fluid in low temperature heat source for power generation. This is, the lack of an exhaustive thermodynamic analysis for this power cycle is the reason why this paper has been developed. The results show the existence of an optimum for

the energy efficiency value as well as for the net specific work for different input temperature values in the turbine.

Nomenclature

A Surface area available for heat transfer, m^2

CDTPC Carbon Dioxide Transcritical Power Cycle

$\dot{E}$ Exergy rate, kW

GWP Global Warming Potential

h Specific enthalpy, kJ/kg

$\dot{I}$ Irreversibility rate, kW

IHX Internal Heat Exchanger

$\dot{m}$ Mass flow, kg/s

wne Net specific work

ODP Ozone Depletion Potential

ORC Organic Rankine Cycle

P Pressure, bar

$\dot{Q}$ Heat flow, kW

state point 1, 2, 2_{is}, 3, 4, 4_{is}

T Temperature, ºC

U Overall heat transfer coefficient, kW/(m^2 ºC)

$\dot{W}$ Power, kW

ΔT_{LM} Log mean temperature difference LMTD, ºC

Subscripts

c Condenser

e Evaporator

ex Exchanger

H Heat source

in Inlet

is Isentropic

L Heat sink

max Maximum

n Net.

out Outlet.

p Pump.

t Turbine.

tot Total

0 Environmental state

Greek symbols

η Efficiency

ρ Density, kg/m^3

1. Description of the carbon dioxide transcritical power cycle.

The CDTPC operation principle is the same as the conventional Rankine cycle but in this case the working fluid is CO_2 instead of water steam. A pump pressurizes the liquid fluid, and it is injected in an evaporator to produce a vapour that is expanded in a turbine connected to a generator; finally, the exit vapour is condensed, starting the new cycle (Fig. 2.a). An Internal Heat Exchanger (IHX) can also be included to increase the energy of the expanded vapour, preheating the pump fluid that will enter the evaporator as shown in Fig. 2.b.

According to the state points shown in the schematic diagram of the simple process in Fig. 2.a, Fig. 3 presents the CO_2 transcritical power cycle in a T-s-diagram plotted with [25] data. As an example, an ideal cycle process is shown by segments that are built from the state points 1, 2_{is}, 3 and 4_{is} marked with (○). The line segment 1-2_{is} represents an isentropic expansion with a production of output work. Heat is extracted from 2_{is} to 3 along a constant subcritical pressure line. Then, an ideal compression of the subcooled liquid from pressure at state point 3 to state point 4_{is} is carried out. Finally, the segment 4_{is}-1 represents the heat addition at constant supercritical pressure to the highest temperature of the cycle at state point 1.

In a real cycle, the expansion and compression processes have certain efficiency, i.e., a real cycle is represented by the segments built from the state points 1, 2, 3 and 4 marked with (○) in the same Fig. 3. In order to increase the process efficiency, an IHX is introduced as in Fig. 2.b, in which a portion of rejected heat, represented by an enthalpy drop from 2 to 2_{IHX} at constant subcritical pressure, is transferred back to the fluid, raising its enthalpy from 4 to 4_{IHX} at constant supercritical pressure. Net heat rejection is indicated by the enthalpy drop from 2_{IHX} to 3 at constant subcritical pressure. State point 3 is at the lowest temperature of the cycle and above the temperature of the heat sink (receiving reservoir). Net input heat to the cycle occurs from 4 (or 4_{IHX}) to 1 at constant pressure. Net work output is the difference between output work from state points 1 to 2 and the input work pump from state points 3 to 4.

2. Modelling of the process.

The equations used to determine the performance of the different CDTPC configurations are presented in this section. Using the first law of thermodynamics, the performance of a CDTPC can be evaluated under diverse working conditions. For both configurations, the analysis assumes the following:

- State: Steady state conditions.
- Loss: No pressure drop or heat loss in the evaporator, condenser, IHX or pipes.
- Efficiencies:
    - Constant isentropic efficiencies of 75% are assumed for the pump as well as for the turbine.
    - The cycle's total energy efficiency is:

$$\eta = \frac{\dot{W}_t - \dot{W}_p}{\dot{Q}_e} \tag{1}$$

where,

$$\dot{W}_t = \dot{m} \times (h_1 - h_2) \tag{2}$$

$$\dot{W}_p = \dot{m} \times (h_3 - h_4) \tag{3}$$

and

$$\dot{Q}_e = \dot{m} \times (h_1 - h_4) \text{ or } \dot{Q}_e = \dot{m} \times (h_1 - h_{4IHX}) \tag{4}$$

5

6

- The exergy efficiency is defined as:

$$\eta_E = 1 - \left(\frac{\sum_i \dot{I}_i}{\sum_i \dot{E}_{in,i}} \right) \tag{7}$$

where I_i is the exergy loss (destruction) of each component i (evaporator, turbine, condenser, pump and IHX) that can be found from an exergy balance:

$$\dot{I}_i = \sum_i \left(1 - \frac{T_0}{T_i} \right) \times \dot{Q}_i + \sum_i \dot{E}_{in,i} - \sum_i \dot{E}_{out,i} - \dot{W}_i \tag{8}$$

The term $\dot{Q}_i$ represents the flow of heat transfer at the location on the boundary where the instantaneous temperature absolute is T_i and the 0 subscripts are relative to the environmental state from which no interaction is possible. Finally, the exergy rate for each state point is expressed as:

$$\dot{E} = \dot{m}[(h - h_0) - T_0(s - s_0)] \tag{9}$$

- Temperatures: An input temperature of the condensation water T_7=15 ºC is considered, so an environmental state T_0=15 ºC is assumed (since no interaction is possible) and a working fluid condensation temperature of T_3=25 ºC. Otherwise, a pinch point of 5 ºC is maintained between T_3 and the output temperature of the condensation water (T_8) for both configurations. In the heating process, the temperature T_i in the high temperature reservoir, i.e. the waste heat of the heat source, can be treated as a constant heat source at T_H. In order to transfer heat, a differential temperature ΔT=20º C is considered and therefore,

$$T_H = T_1 + \Delta T_H \tag{10}$$

  In the condensation process, the temperature T_i is the temperature of the low-temperature reservoir T_L. This temperature is considered to be equal to $T_L = T_7$.

- Conditions: Each turbine input temperature previously studied has been maintained constant (T_1=60 ºC, 90 ºC, 120 ºC and 150 ºC) from a turbine input pressure P_1=66 bar until the net work at around zero ($\dot{W}_n = \dot{W}_t - \dot{W}_p \cong 0$) is achieved for the case of the simple cycle, and also with a temperature difference (ΔT) between T_2 and T_4 of at least 5 ºC for the cycle with IHX. The outlet pressure P_2 in the turbine was always 65 bar.

The thermodynamic analysis of the CDTPC was performed using a process simulator HYSYS® (Hyprotech Co., Canada). This simulator is useful for thermodynamic analysis, especially steady state condition, and has the advantage of including fluid properties and ready to use optimization tools. Its predictions have been compared with the ones from [25] and the results are very similar. The simulation flow diagram is the same as that presented in Fig. 2 and the method for resolving every one of its components is the following:

- Turbine: the efficiency of a turbine is given as the ratio of the actual power produced ($\dot{W}_t$) in the expansion process to the power produced for an isentropic expansion ($\dot{W}_{t,is}$) :

$$\eta_t = \dot{W}_t \Big/ \dot{W}_{t,is} \times 100\% \tag{11}$$

With the inlet and outlet pressures, the inlet temperature and the efficiency known, the software calculates the expansion rigorously following the isentropic line from the inlet to outlet pressure. Using the enthalpy at that point, as well as the specified efficiency, the software determines the actual outlet enthalpy. From this value and the outlet pressure, the outlet temperature is determined.

- Pump: Calculations are based on the standard pump equation for power, which uses the pressure rise, the liquid flow rate and density:

$$\dot{W}_{p(ideal)} = \left(P_4 - P_3\right) \times \dot{m} \Big/ \rho_{liquid} \tag{12}$$

The equation (12) defines the ideal power needed to raise the liquid pressure and the actual power requirement of the pump is defined in terms of the pump efficiency:

$$\eta_p = \dot{W}_{p(ideal)} \Big/ \dot{W}_{p(actual)} \times 100\% \tag{13}$$

When the efficiency is less than 100%, the excess energy goes into raising the temperature of the outlet stream. However, for a pump, an efficiency of 100% does not correspond to a true isentropic compression of the liquid.

Combining (12) and (13) leads to the following expression for the actual power requirement of the pump:

$$\dot{W}_{p(actual)} = \left(P_4 - P_3\right) \times \dot{m} \times 100\% \Big/ \left(\rho_{liquid} \times \eta_p\right) \tag{14}$$

- Heat exchangers: The Heat Exchanger calculations are based on energy balances for hot and cold fluids:

$$\dot{m}_{cold} \times \left(h_{out} - h_{in}\right)_{cold} = \dot{m}_{hot} \times \left(h_{in} - h_{out}\right)_{hot} \quad (15)$$

and the total heat transferred between the tube and shell sides (Heat Exchanger duty) can be defined in terms of the overall heat transfer coefficient, the area available for heat exchange, and the log mean temperature difference:

$$\dot{Q}_{ex} = U \times A \times \Delta T_{LM} \quad (16)$$

where:

$$\Delta T_{LM} = \frac{\Delta T_1 - \Delta T_2}{\ln\left(\Delta T_1 / (\Delta T_2)\right)} \quad (17)$$

and:

$$\Delta T_1 = T_{hot,in} - T_{cold,out} \quad (18)$$

$$\Delta T_2 = T_{hot,out} - T_{cold,in} \quad (19)$$

In our case, the condenser and IHX require more detailed explanations due to the special conditions of the CDTPC studied. Indeed, the traditional definition of its effectiveness and the LMTD methods, which is based on the assumption of constant specific heat, cannot be used because, for the CO_2, this property varies considerably with the temperature near the critical state and in general, for the case of supercritical fluids according to [14] . Based on this observation, a method is needed for calculating the interchanges, taking into account this variation in the properties of the supercritical CO_2. The “weighted model” method provided by the software used is an excellent model to deal with non linear heat curve problems such as the phase change of pure components in one or both heat exchanger heat sides. With the weighted model, the heating curves are broken into intervals, and an

energy balance is performed along each interval. An LMTD and UA are calculated rigorously for each interval in the heat curve, and summed to calculate the overall exchanger UA. Furthermore, when this method is selected, it is possible to use the function “auto interval”, which determines where points should be added to the heat curve, making the calculations until the lowest number of intervals and a minimum mistake value are obtained. The results obtained with this method are similar to those achieved in [14,23], which discretize the heat exchangers, the variation in properties being very small in each step, allowing an average constant value, different for each step, to be taken. However, unlike in the present work, they simplified the calculation of the LMTD using the difference between the mean temperatures of each step.

The weighted model is available only for counter current exchangers, and it is essentially an energy and material balance model. Other methods of this software, such as the “end point model”, treat the heat curves for both Heat Exchanger sides as linear. For simple problems, where there is no phase change and Cp is relatively constant, this option may be sufficient to model the Heat Exchanger: For non-linear heat flow problems the weighted model should be used instead.

- Evaporator: For the calculation of the cycle performance, it is only necessary to know how much energy is required to heat the process flow directed to the turbine. Because it is not our objective to study the conditions of the utility itself, that's why it is used the available evaporator in the software in which the inlet stream to the evaporator is heated to the required outlet conditions i.e., until the conditions established in the turbine entrance and according to the Fig. 2, the energy stream, $\dot{Q}_e$ provides the enthalpy difference between the two streams.

3. Results and discussion.

This section presents the results obtained in the simulations carried out. The procedure for analyzing the behaviour of the CDTPC consisted of varying the input pressure to the turbine from 1 bar over the discharge pressure (65 bar) until the net work was nearly zero or until pressure and temperature conditions no longer allowed the fluid to be in a gaseous state for injection to the turbine. This was done by maintaining each of the evaluated temperatures (60 ºC, 90 ºC, 120 ºC and 150 ºC) constant. Furthermore, this analysis took into account the effect of adding an IHX to the cycle until its presence was justified, i.e., until T_2-T_4 was below 5 ºC for each of the four temperatures studied.

3.1 Energy analysis.

Results achieved in the simulations carried out are shown in Figs. 4 and 5. The blue tendency lines and the open blue symbols indicate the energy efficiencies of the simple cycle, the green tendency lines and the green bold symbols point to the energy efficiencies of the cycle with IHX and the discontinuous red lines represent the net specific work (*wne)*. On the other hand, symbols represented with a triangle (▲), square (■), circle (●) and rhombus (♦) are linked with the analyzed temperatures of 150 ºC, 120 ºC, 90 ºC and 60 ºC, respectively. The curves obtained in Figs. 4 and 5 conform to the type $y = a + b \times P_1 + c \times P_1^2$, where "$y$" refers to *wne* or *η*. The coefficients and the R^2 for these equations are presented in Table 1.

A glance at Figs. 4 and 5 shows a parabola-like behaviour and thus the existence of a maximum for both the *η* and the *wne* at all four temperatures. There are several reasons for this: first, noting that the input temperature and the discharge pressure of the turbine are fixed; second, we assume that the work produced by this device is that given by (2); third, as can be seen in Fig. 3, for a constant temperature, when the pressure increases, Δh rises, and $\dot{W}_t$

along with it, which ensures the increase of both *η* and the *wne* of the cycle. The above is true until, due to the thermodynamic properties of each particular fluid, a maximum pressure value appears for *η* and *wne* separately, in which the work done by the pump becomes appreciable, decreasing the *wne*, and therefore decreasing the energy efficiency of the cycle as the variable pressure rises, as in [23].

As discussed previously, the work of expansion increases as the input pressure to the turbine increases. However, the necessary pumping work also rises, as can be seen in Fig. 6 (in which only the results obtained for the simple cycle with T_1=150 ºC are shown, since its behaviour is similar to that of the rest of the analyzed cases). The approximation equations and correlation coefficients of the curves presented at Fig. 6 are $\dot{W}_t = -26.55 + 0.558 \times P_1 - 0.001012 \times P_1^2$ with R^2= 97.6% and $\dot{W}_p = -13.345 + 0.205299 \times P_1$, with R^2= 100.0%, respectively.

A rigorous analysis of Fig. 6 allows us to see that the rate of increase in the work produced by expansion is higher than the rate of increase in the necessary work for the pump, e.g., for P_1=130 bar, 0.3 kW/bar is produced, whereas 0.2 kW/bar are essential for the pump. This is true until, at a particular pressure value (in this case, P_1≈150 bar), the rate of increase in the values of the pump work exceed those of the expansion work, and consequently, the *wne* begins to decrease, i.e., for a pressure P_1=170 bar, 0.15 kW/bar is produced, while 0.2 kW/bar is required by the pump. This behaviour, of the existence of a maximum for the *wne*, is similar to that found in [14,16,23].

However, the fact that the pressures which make the *η* maximum and the *wne* are different is related to the variation of $\dot{Q}_e$, something which is necessary to achieve the imposed turbine input conditions. Figure 7 analyzes this behaviour and as expected, the $\dot{Q}_e$ decreases as the input pressure to the turbine increases for the simple cycle. This is due to the rise in the outlet temperature of

the pump (because of the heat given off by the pump inefficiencies), and therefore the entrance to the evaporator, which supposes a lower heat transfer requirement. As in the case of the simple cycle, the rise in input pressure to the turbine for the cycle with IHX causes a decrease in the output temperature of the fluid in the turbine and an increase in the output temperature of the pump. Thus, progressively less heat can be used in the IHX, requiring an increase in the heat to be applied in the evaporator. On the other hand, this $\dot{Q}_e$ for the cycle with IHX is always less than the simple cycle for any pressure P_1 and for each temperature evaluated as can be seen in Fig. 7. In addition, it is worth noting that in this same Fig. 7, the tendency is similar and the difference is not very appreciable in the values of the curves for the case of the cycle with IHX. This is because, for the same pressure, the outlet temperature of the cold side (T_{4IHX}) of this heat exchanger differs by only a few degrees in each of the evaluated temperatures. For the curves obtained in the Fig. 7, the parameters of adjustment equations conform to the type $\dot{Q}_e = a + b \times P_1 + c \times P_1^2$, with their corresponding correlation coefficients, are presented in the Table 2.

Figs. 4, 5, 6 and 7 show that, depending on the inclusion or not of an IHX, the benefits from the input temperature of the turbine and the design criteria for the chosen cycle (maximum *η*, maximum *wne* or a value between both) are different. A more exhaustive analysis of this appreciation is explained in the following sections. However, only the results obtained for T_1=150 ºC are commented on in sections 3.1.1 and 3.1.2, due to the similar behaviour with the rest of analyzed cases.

3.1.1 Effect on the maximum energy efficiency (η_{max}) and the net specific work (wne) of the cycle with the inclusion of an IHX.

According to the results presented in Fig. 4 and taking the η_{max} as the base criteria of design, i.e. comparing the maximum obtained values of the energy efficiency when an IHX is incorporated versus the simple cycle, an increase in the efficiency of 1.7% (passing from 8.1% to 9.8%, i.e., 21% more) can be

appreciated. The *wne*, meanwhile, increases by 0.4 kJ/kg, (passing from 17.5 to 17.9, i.e., 2.3% more). Therefore, and according to the remarks in [14,16], including an IHX increases the energy efficiency of the cycle. However, that value greatly depends on the input temperature to the turbine, as will be explained in a later section.

3.1.2 Effect on the energy efficiency (η) of the cycle with the inclusion of an IHX based on the design criteria for a maximum net specific work (wne_{max}).

In this case, and according to the results presented in the same Fig. 4, if the priority of the design is to obtain the maximum work, which occurs at P_1=150 bar, adding an IHX causes an increase in η of 1.8% (from 7.8% to 9.6%, i.e., 23%).

In the same way, when η_{max} (obtained with the IHX) and the η (achieved with the conditions that make wne_{max}) are compared, a percentage decrease of only 0.2%, (i.e., 2% less) can be appreciated for the evaluated temperature of 150 ºC. Likewise, doing this same comparison for the energy efficiency without IHX, the decrease is 0.3% (i.e., 3.8% less). Clearly, a very low reduction of η has been achieved when compared with that obtained with the condition of wne_{max} and of η_{max} for both cases (with IHX, 2% as maximum, and without IHX, 3.8% as maximum). Furthermore, as happens with the criterion of design based on η_{max}, the inclusion of IHX increases the η of the cycle, which depends on temperature achieved at the input of the turbine.

3.1.3 Effect of the input temperature to the turbine taking η_{max} as design criterion.

An analysis of the effect that the input temperature of the turbine has, when taking the maximum energy efficiency of the system as base criterion, shows how both η and the *wne* rise sharply in line with the increase of temperature (a similar behaviour can be inferred from the results in [23]). For the case of the simple cycle, the effect of increasing the temperature from 60 ºC to 90 ºC, from

90 ºC to 120 ºC and from 120 ºC to 150 ºC, is to raise the η by 2.1%, 1.9% and 1.6% (i.e., 84%, 41.3% and 24.6% more) and the *wne* by 4.1 kJ/kg, 4.6 kJ/kg and 5.5 kJ/kg (i.e., 124.2%, 62.1% and 45.8% more), respectively. However, this supposes an increase in the pressure of the system by 25 bar, 25 bar and 27 bar, respectively; with both the technical and the economic problems that this would entail.

Likewise, under the same considerations but for the case of the cycle with IHX, the increase of the input temperature to the turbine from 60 ºC to 90 ºC, from 90 ºC to 120 ºC and from 120 ºC to 150 ºC causes an increase of the maximum energy efficiency of the system of 2.5%, 2.4% and 2.5% (i.e., 104.1%, 48.9% and 34.2% more) and of the *wne* by 4.1 kJ/kg, 5.1 kJ/kg and 5.3 kJ/kg (i.e., 120.5%, 48.9% and 34.2% more), respectively. The pressure must also increase by 17 bar, 16 bar, 12 bar, in this order. In conclusion, increasing the input temperature to the turbine from 60 ºC to 150 ºC, for the case of the simple cycle, causes an increase of the energy efficiency of 5.6% (i.e., 224% more) and of the *wne* of 14.2 kJ/kg (i.e., 430% more); whereas, for the cycle with IHX, this increase is of 7.4% (308% more) and 14.5 kJ/kg (426% more), respectively.

3.1.4 Effect of the input temperature to the turbine taking the wne_{max} as base criterion of design.

If the analysis is done with the criteria of wne_{max}*.,* the effect of increasing the temperature from 60 ºC to 90 ºC, from 90 ºC to 120 ºC and from 120 ºC to 150 ºC raises the wne_{max} for the case of the simple cycle by 4.3 kJ/kg, 5.0 kJ/kg and 5.4 kJ/kg (i,e., 122.8%, 64.1%, 42.1% more) respectively; whereas the η rises by 2%, 1.8% and 1.6% (i.e., 79.5%, 40.9%, 25.8% more) and with requirements of a pressure increase of 18 bar, 20 bar and 22 bar, in this order. Under the same design premises, for the case of the cycle with IHX, the increase of input temperature to the turbine, the wne_{max} and the pressure are evidently equal to those presented in the simple cycle. However, η increases by 2.4% for each of the three temperature levels studied (i.e., 100%, 50% and 33.3% more). In short, starting with the design criterion of wne_{max} and for the cycle with and

without IHX, the increase of input temperature to the turbine from 60 ºC to 150 ºC supposes an increase of the wne_{max} by 14.7 kJ/kg (i.e., 420% more); likewise, the η for the case of the simple cycle rises by 5.4% (i.e. 218.3% more) and for the cycle with IHX by 7.2% (i.e., 300% more).

According to the above remarks, the effect of increasing the input temperature to the turbine, whenever possible, supposes a sharp increase of both η and the *wne* in the system for both configurations, with and without IHX. Furthermore, it is known that the inclusion of the IHX causes an increase of the energy efficiency cycle, but other aspects of these results as the raise of the capital cost of the overall system and the complexity of the flow scheme will have to be analyzed deeply in future works. In the same way, an analysis of a CDTPC has not been reported in the literature with optimization tools for the achievement of a higher efficient through process integration, e.g, by means of a pinch analysis. Moreover, and because of the CDTPC proposed can work with low enthalpy heats, coming from waste heats of processes or from low-calorific value fuels burning, other interested researches to approach in the future, will have to study the full plant of power generation.

3.2 Exergy analysis.

The work fluid tends to continually increase the temperature in the evaporator because, when it is over the critical point, there is no coexistence between the liquid and gaseous phases in a range of temperatures. Thus, for the supercritical cycle, fewer and more uniform differences of temperatures with respect to the thermal source will be produced, causing an important reduction in the irreversibility, as well as an increase in the mean temperature of heat acceptance and therefore of the thermal and exergy yield. Furthermore, the results obtained in the previous section, showing the non-existence of an operation point that produces a maximum, at the same time, of both efficiency and specific net work, make the use of other criteria (such as the exergy) or an analysis that reasonably optimizes and/or involves both parameters

indispensable. Thus, an exergy analysis of the process has been carried out on the basis of the results obtained from the simulations using both the model and the suppositions and parameters mentioned in section 2. However, the procedure used to analyze the behaviour of the CDTPC was the same as that mentioned in section 3.1, whose results are shown in Figs. 8 and 9.

Some figures have been made by means of graphs to analyze what happens in each of the devices that make up the cycle when the input pressure to the turbine increases beyond the irreversibility of the process, in percentages and kW, for both the simple cycle (a and b) as well as those with an IHX (c and d). However, in Figs. 8.a, b, c and d, only the results for 150 ºC are represented as input temperature to the turbine. This is due to the similar behaviour for the rest of the temperatures evaluated. For the curves obtained in the Fig. 8, the parameters of adjustment equations conform to the type $\dot{I} = a + b \times P_1 + c \times P_1^2$, with their corresponding correlation coefficients, for the cycles without and with IHX are presented in the Table 3 and 4, respectively.

Figs. 8.a and b show that when the input pressure to the turbine increases, the irreversibility of the heat flow in the evaporator, as well as in the condenser, decreases, while those of the turbine and pump rise. The explanation for this is related to the rise in the temperature of the fluid in the pump outlet when a higher discharge pressure is imposed on the pump (and therefore on the input pressure to the turbine). This causes the irreversibility by heat flow in the evaporator to decrease when the temperature of the fluid approaches the temperature of the heat source (a hypothesis in keeping with that explained in [26]). The same happens with respect to the condenser when a lower discharge temperature is produced. However, the increase of the destruction of exergy by work is less than that of these exchangers, and hence the destruction of total exergy decreases in line with the increase in the input pressure to the turbine, being more appreciable at pressures below 150 bar, as shown in Fig. 8.b.

Under the same suppositions, an analysis has been carried out of the cycle with IHX whose results are presented in Figs. 8.c and d. Evidently, the incorporation of an IHX causes a considerable decrease in the destruction of exergy in the condenser, due to the decrease in the heat flow needed to extract the fluid. This is because it has already exchanged the heat previously in the IHX and therefore, this is the last device where the majority of the destruction of the exergy by heat flow is produced (together with the evaporator). Nevertheless, as the input pressure to the turbine increases, the irreversibility in the IHX decreases sharply because of the increase of the temperature of the fluid discharged by the pump. The output temperature of the turbine also decreases, and therefore, the heat transfer in this exchanger too. In conclusion, the heat flow needed in the evaporator to bring the fluid to the design condition of 150 ºC increases and, therefore, the destruction of exergy in this device.

In general, it can be said that, when the input pressure to the turbine increases in the case of the cycle with IHX, the exergy destroyed rises gently (Fig. 8.d). However, the addition of this device causes a decrease of between 20-60% in the irreversibility when compared with those generated in the simple cycle, as indicated in Figs. 8.b and d.

The results obtained when the turbine input pressure increases over the exergy efficiency of the process with and without IHX, and for the different evaluated temperatures, are presented in Fig. 9. As can be observed, unlike the energy efficiency, the exergy efficiency has no maximum, but while the operation pressure of the process rises, the exergy efficiency also increases, for both the simple cycle (with similar results to those mentioned in [14]) and the cycle with IHX. However, it can be concluded that, depending on the addition of an IHX and on the turbine input temperature and pressure, there can be differences in the value of the exergy efficiency; hence, they can condition the design criterion of the chosen cycle in the obtaining of a maximum energy efficiency or a maximum net specific work. The curves obtained in Fig. 9 also fit quite well to

the form $\eta_E = a + b \times P_1 + c \times P_1^2$. The coefficients and the R^2 for these equations are shown in Table 5.

3.2.1 Effect of the input temperature to the turbine on the exergy efficiency (η_E).

Figure 9 shows that, for both the case of the simple cycle and for that of the IHX and with a specific pressure, the increase in the input temperature to the turbine causes a decrease of the exergy efficiency of the cycle as a result of the increase of irreversibility due to the rise in heat flow required. For example, at a pressure of 150 bar, and two different turbine input temperatures of 120 ºC and 150 ºC, the exergy efficiency decreases by 10% (a change from 40% to 36%, respectively).

For the cycle with IHX, this effect stops being perceptible for pressures over 100 bar, while for lower pressures it causes a very appreciable decrease in the exergy efficiency of the process, e.g., at a pressure of 80 bar and two turbine input temperatures of 120 ºC and 150 ºC, the exergy efficiency decreases by 3.5% (a change from 29% to 28%, respectively). However, when the highest and lowest temperatures to be analyzed in the present study (i.e., a change from 150 ºC to 60 ºC) are compared at the same pressure, the exergy efficiency increases by 20% (a change from 28% to 35%). This is due to the low variation in the heat flow required to evaporate the CO_2 (and hence of the irreversibility), due to the heat recovery by the IHX.

3.2.2 Effect of the input pressure to the turbine on the exergy efficiency (η_E).

When a high discharge pressure is imposed on a pump (and therefore on the turbine input), the output temperature of the work fluid rises, causing a decrease in the irreversibility by heat flow in the evaporator, as the temperature of this fluid approaches that of the heat source. Hence, an increase of the input pressure to the turbine, for both the simple cycle and that with IHX, causes an increase in the exergy efficiency, as presented in Fig. 9. Its behaviour tends to be asymptotic (even more so for the case of the cycle with IHX), the maximum

of the temperatures of 90 ºC, 120 ºC and 150 ºC being around 50%. For the temperature of 60 ºC, however, it is limited by its maximum operating pressure to 40%. Nevertheless, a decrease in the input temperature to the turbine causes a decrease in the sensitivity of the process in relation with the exergy efficiency (and much lower for the cycle with IHX). In other words, the lower the input temperature to the turbine, the lower the gain in exergy efficiency for a short increase of pressure. This effect decreases whenever it approaches the value of its asymptote in each case. For instance, in the case of a simple cycle and that with IHX, an increase of 20 bar (from 80 to 100 bar) and for the temperature of 150 ºC, causes an increase in the exergy efficiency of 110% (a change from 10% to 21%) and of 42% (a change from 28% to 40%), respectively. While the same increase of pressure for the temperature of 90 ºC produces an increase of 87% (a change from 15% to 28%) for the case of simple cycle and 35% (a change from 31% to 42%) for the cycle with IHX.

3.2.3 Effect of the inclusion of an IHX on the exergy efficiency (η_E).

Evidently, the inclusion of an IHX causes an important decrease of heat flow required in the process and therefore also of the irreversibility (see Figs. 8.c and d). Thus, for a same input pressure to the turbine, the inclusion of an IHX causes an increase of up to 200% in the exergy efficiency, a difference that effectively decreases as the input pressure to the turbine increases for all the temperatures studied, as can be seen in Fig. 9. For instance, for the temperature of 150 ºC and a pressure of 80 bar, the inclusion of an IHX causes an increase of 180% (a change from 10% to 28%) in the value of the exergy efficiency; while, for the same temperature and a pressure of 100 bar, the increase drops to 90% (a change from 21% to 40%). Thus, the increase in the exergy efficiency when an IHX is introduced drops, when the input temperature of the turbine decreases. For example, for the same input pressure to the turbine of 80 bar, but with an input temperature of 60 ºC, the exergy efficiency increases by only 84% (a change from 19% to 35%).

3.3 Optimum conditions of design.

According to the results presented in the previous sections, the mean values of the maximum pressures for the energy efficiency, as well as for the net specific work for each of the temperatures studied, have been considered as optimum design conditions, irrespective of whether the IHX is included or not. These results are shown in Table 6, where the values of net specific work and the energy and exergy efficiency corresponding to this optimum pressure point are included. If they are compared with the maximum values achieved for these parameters, a decrease in the energy efficiency of 0.15% is obtained as maximum, (equivalent to 2.3%); while, for the case of the *wne*, it decreases by only 0.3 kJ/kg as maximum (also equivalent to only 2.3%). However, as the exergy efficiency is always increasing, having a mean design point causes a decrease, or an increase, of around 2% as maximum (equivalent to 6%). This depends on the point of comparison, either $\eta_{\max}$ or wne_{max}, and also on the presence of the IHX (due to the location to the right of the maximum energy efficiency point with regard to the maximum point of the *wne* for a simple cycle and to the left for the cycle with IHX, as can be seen in Figs. 4 and 5). In other words, for a simple cycle, the η_E decreases if it is compared with the one obtained for η_{max}, and increases if it is related with the wne_{max}. Further, when the IHX is included, the behaviour is the opposite.

Conclusions.

Considering the energy analysis carried out, the existence of an optimum maximum for the energy efficiency, as well as for the specific net work, is obvious. Additionally, it can be seen how the increase of the input temperature to the turbine supposes an increase in the value of such parameters for both configurations with and without IHX. However, there is no operation point that produces, at the same time, a maximum in terms of efficiency and specific net work; hence, the use of other criteria is indispensable for deciding between these options or for imposing an intermediate value of pressure that reasonably balances both parameters. The exergy efficiency, however, does not present a

maximum. It does increase, nevertheless, in line with the increase in the operation pressure of the process, in both the simple cycle and that with IHX. Furthermore, differences in the values of the exergy efficiency are observed, depending on whether or not an IHX is included and on the input temperature and pressure to the turbine. This can condition the design criterion for the selected cycle for obtaining a maximum efficiency or a maximum *wne*.

Based on the simulations carried out, it can be concluded that the CDTPC is suitable for the production of useful energy using low enthalpy heat, as it is possible to operate in relatively low temperature ranges. In addition, many of the aspects taken into account nowadays in these processes, such as environmental issues, safety and efficient and rational use of energy are satisfied. However, the real application of the proposed cycle depends strongly on the cost of the equipment for the high pressures required for its operation.

Acknowledgements.

Support for this work came from the Spanish Ministry of Education project ENE2009-14644-C02-01. The authors gratefully acknowledge all the invaluable comments of Ing. Cecilia Sanz from the CARTIF Foundation. Furthermore, F.V. thanks the scholarship awarded by the “Programa Iberoamericano de Ciencia y Tecnología para el Desarrollo”, CYTED, the Cartif Foundation and the University of Valladolid in the realization of his doctoral thesis, on which this paper is based.

References

[1] Fredy V, Gregorio A, José S, Farid C. Tecnología ORC como potenciador de las energías no convencionales en zonas no interconectadas y aumento de la eficiencia energética en la industria. Proceedings of the 1st World Congress & Exhibition Engineering; 2010 October 17th–20th; Buenos Aires, Argentina.

[2] Fredy V, Gregorio A, Farid C, Carlos V. “Selección del fluido de trabajo en los sistemas de cogeneración ORC”. Proceedings of the VI International Conference of Renewable Energie. Saving Energy and Energy Education; 2009 June 9-12; La Habana, Cuba.

[3] Yamamoto T, Furuhata T, Arai N, Mori K. Design and testing of the organic Rankine cycle. Energy 2001; 26: pp 239–251.

[4] Hung T.C, Shai T.Y, Wang S.K. A review of organic Rankine cycles (ORC`s) for the recovery of low-grade waste heat. Energy 1997; 22 (7): 661-667.

[5] Desai N.B, Bandyopadhyay S. Process integration of organic Rankine cycle. Energy 2009; 34: 1674–1686.

[6] Chen Y, Lundqvist P, Johansson A, Platell P. A comparative study of the carbon dioxide transcritical power cycle compared with an organic rankine cycle with R123 as working fluid in waste heat recovery. Applied Thermal Engineering 2006; 26: 2142–2147.

[7] Hung T.C, Wang S.K, Kuo C.H, Pei B.S, Tsai K.F. A study of organic working fluids on system efficiency of an ORC using low-grade energy sources. Energy 2010; 35: 1403–1411.

[8] Manolakos D, Kosmadakis G, Kyritsis S, Papadakis G. Identification of behaviour and evaluation of performance of small scale, low-temperature Organic Rankine Cycle system coupled with a RO desalination unit. Energy 2009; 34: 767–774.

[9] Vaja I, Gambarotta A. Internal Combustion Engine (ICE) bottoming with Organic Rankine Cycles (ORCs). Energy 2010; 35: 1084–1093.

[10] Wang H, Peterson R, Harada K, Miller E, Ingram G.R, Fisher L, Yih J, Ward C. Performance of a combined organic Rankine cycle and vapor compression cycle for heat activated cooling. Energy 2011; 36: 447-458.

[11] Rosyid H, Koestoer R, Putra N, Nasruddin, Mohamad A, Yanuar. Sensitivity analysis of steam power plant-binary cycle. Energy 2010; 35: 3578-3586.

[12] Lai N.A, Wendland M, Fischer.J. Working fluids for high-temperature organic Rankine cycles. Energy 2011; 36: 199-211.

[13] Roy J.P, Mishra M.K, Misra A. Parametric optimization and performance analysis of a waste heat recovery system using Organic Rankine Cycle. Energy 2010; 35: 5049-5062.

[14] Cayer E, Galanis N, Desilets M, Nesreddine H, Roy P. Analysis of a carbon dioxide transcritical power cycle using a low temperature source. Applied Energy 2009; 86: 1055–1063.

[15] Chen H, Goswami D.Y, Rahman M.M, Stefanakos E.K. A supercritical Rankine cycle using zeotropic mixture working fluids for the conversion of low-grade heat into power. Energy 2011; 36: 549-555.

[16] Chen Y, Pridasawas W, Lundqvist P. Dynamic simulation of a solar-driven carbon dioxide transcritical power system for small scale combined heat and power production. Solar Energy 2010; 84: 1103–1110.

[17] Schuster A, Karellas S, Aumann R. Efficiency optimization potential in supercritical Organic Rankine Cycles. Energy 2010; 35: 1033–1039.

[18] Yamaguchi H, Zhang X.R, Fujima K, Enomoto M, Sawada N. Solar energy powered Rankine cycle using supercritical CO_2. Applied Thermal Engineering 2006; 26: 2345–2354.

[19] U.S. Environmental Protection Agency Class I Ozone - Depleting Substances [internet]. Washington D.C. – Available at: <www.epa.gov/ozone/science/ods/classone.html>. [accessed 15.08.2010].

[20] Intergovernmental Panel of Climate Change (IPCC), working group I. Climate change 2001: The scientific Basis. Third assessment report.

[21] Zhang X.R, Yamaguchi H, Uneno D. Theoretical analysis of a thermodynamic cycle for power and heat production using supercritical carbon dioxide. Energy 2007; 32(4): 591–599.

[22] Zhang X.R, Yamaguchi H, Uneno D. Experimental study on the performance of solar Rankine system using supercritical CO_2. Renewable Energy 2007; 32: 2617–2628.

[23] Cayer E, Galanis N, Nesreddine H. Parametric study and optimization of a transcritical power cycle using a low temperature source. Applied Energy 2010; 87: 1349–1357.

[24] Zhang X.R, Yamaguchi H, Uneno D, Fujimab K, Enomotoc M, Sawadad N. Analysis of a novel solar energy-powered Rankine cycle for combined power and heat generation using supercritical carbon dioxide. Renewable Energy 2006; 31: 1839–1854.

[25] Lemmon E.W, Huber M.L, Mclinden M.O. Reference fluid thermodynamic and transport properties (REFPROP). NIST Standard Reference Database 23, Version 8.0; 2007.

[26] Hung T.C. Waste heat recovery of organic Rankine cycle using dry fluids. Energy Conversion and Management 2001; 42: 539-553.

TABLES

Table 1. Coefficients and R^2 for curves *η* and *wne* according to Figs. 4 and 5 and for the temperatures studied.

Table 2. Coefficients and R^2 for curves $\dot{Q}_e$ according to Fig. 7 and for the temperatures studied.

Table 3. Coefficients and R^2 for $\dot{I}$ curves according to Fig. 8.a and b.

Table 4. Coefficients and R^2 for $\dot{I}$ curves according to Fig. 8.c and d.

Table 5. Coefficients and R^2 for η_E curves according to Fig. 9 and for the temperatures studied.

Table 6. Optimum conditions of design.

Table 1.

Coeff.	Temperature (ºC)											
	150			120			90			60		
	η without IHX	η with IHX	*wne*	η without IHX	η with IHX	*wne*	η without IHX	η with IHX	*wne*	η without IHX	η with IHX	*wne*
a	-8.504	-20.48	-13.20	-11.46	-23.94	-18.16	-16.46	-29.63	-25.28	-25.01	-6.774	- 40.10
b	0.1816	0.4239	0.3527	0.2366	0.5133	0.4163	0.3506	0.6685	0.5614	0.5904	0.1080	0.9656
c	-0,000495	-0.001457	-0.001012	-0.000780	-0.002085	-0.001422	-0.001460	-0.003226	-0.002407	-0.003167	-	-0.005343
R^2 (%)	97.1	95.1	87.7	98.3	97.6	89.6	99.7	99.3	94.2	100.0	94.3	99.6

Table 2.

Coeff.	Temperature (ºC)							
	150		120		90		60	
	without IHX	with IHX	without IHX	with IHX	without IHX	with IHX	without IHX	with IHX
a	349.9	43.35	326.2	29.34	302.1	14.31	242.2	68.91
b	-0.8895	1.579	-1.069	1.881	-1.241	2.275	-0.4183	0.8888
c	0.000694	-0.004010	0.000893	-0.005772	0.000574	-0.008457	-0.007676	-
R^2 (%)	100.0	99.6	100.0	99.8	100.0	100.0	100.0	99.5

Table 3.

Coeff.	$\dot{I}_e$		$\dot{I}_c$		$\dot{I}_t$		$\dot{I}_p$	
	(kW)	(%)	(kW)	(%)	(kW)	(%)	(kW)	(%)
a	93.41	73.91	52.37	45.80	-7.232	-15.08	-2.964	-4.623
b	-0.5139	-0.1138	-0.3392	-0.1854	0.1464	0.2494	0.04240	0.04986
c	0.000843	-0.000109	0.000615	0.000236	-0.000233	-0.000301	0.000031	0.000173
R^2 (%)	99.2	99.8	98.7	99.9	99.5	99.9	100.0	99,8

Table 4.

Coeff.	$\dot{I}_e$		$\dot{I}_c$		$\dot{I}_t$		$\dot{I}_p$		$\dot{I}_{IHX}$	
	(kW)	(%)*	(kW)	(%)	(kW)	(%)	(kW)	(%)	(kW)	(%)
a	4.275	- 67,26	-0.4796	-3.088	-9.883	-29.73	-2.673	-9.633	56.02	140.7
b	0.2439	2,645	0.01497	0.07955	0.1894	0.5889	0.03764	0.1588	- 0.6634	-1.663
c	-0.000708	- 0,01774	0.000050	-0.000093	-0.000389	-0.001583	0.000049	-0.000208	0.001962	0.004904
R^2 (%)	94.0	98.5	100.0	99.9	99.9	99.8	100.0	100.0	98.3	98.7

* $+ 0.000038 \times P_1^3$

Table 5.

Coeff.	Temperature (ºC)							
	150		120		90		60	
	without IHX	with IHX	without IHX	with IHX	without IHX	with IHX	without IHX	with IHX
a	-28.81	-61.94	-44.32	-87.24	-72.34	-136.9	-146.1	-49.42
b	0.5876	1.426	0.8566	2.028	1.411	3.263	3.086	1.037
c	-0.001080	-0.004476	-0.001950	-0.007598	-0.004201	-0.01468	-0.01285	-
R^2 (%)	98.2	96.9	98.8	98.5	99.6	99.6	100.0	98.0

Table 6.

Parameter	Temperature (ºC)							
	150		120		90		60	
	With IHX	Without IHX	With IHX	Without IHX	With IHX	Without IHX	With IHX	Without IHX
Pressure [bar]	141	161	124	136.5	106	114	88.5	92.5
η [%]	9.8	8.0	7.3	6.4	4.8	4.5	2.4	2.5
η_E [%]	48	38	46	36	43	34	40	30
nsw [kJ/kg]	18.1	18	12.6	12.5	7.7	7.6	3.5	3.4

FIGURES

Fig. 1. Schematic diagram of the temperature variation between heat source (- - -) and working fluid (——) in the counter current evaporator for azeotrope or single fluid, zeotrope and supercritical process, respectively.

Fig. 2. Schematics diagram of the process simple (a) and with IHX (b). (t) Turbine, (c) Condenser, (p) Pump, (e) Evaporator, (ex) Internal Heat Exchanger.

Fig. 3. T-s Diagram for differents CO_2 transcritical power cycles.

Fig. 4. Energy efficiency (η) with IHX (▲) and without IHX (Δ), and net specific work (*wne*) produced vs. Pressure P_1 for T_1=150 ºC.

Fig. 5. Energy efficiency (η) with IHX (bold symbols) and without IHX (open symbols), and net specific work (*wne*) produced (discontinuos lines) vs. Pressure P_1 for T_1=120 ºC (square), 90 ºC (circle), and 60 ºC (rhombus).

Fig. 6. Work produced and consumed by the turbine and the pump, respectively vs Pressure P_1 at T_1=150 ºC, without IHX.

Fig. 7. Heat required in the evaporator vs. input pressure to the turbine P_1 for each one of the temperatures studied in the cycle with and without IHX.

Fig. 8. Effect of the input pressure in the turbine over the irreversibilities of the process in an input temperature to the turbine at 150 ºC for the cycle without IHX (a), (b) and for the cycle with IXH (c), (d).

Fig. 9. Exergy efficiency vs Pressure P_1 with and without IHX and for the studied temperatures.

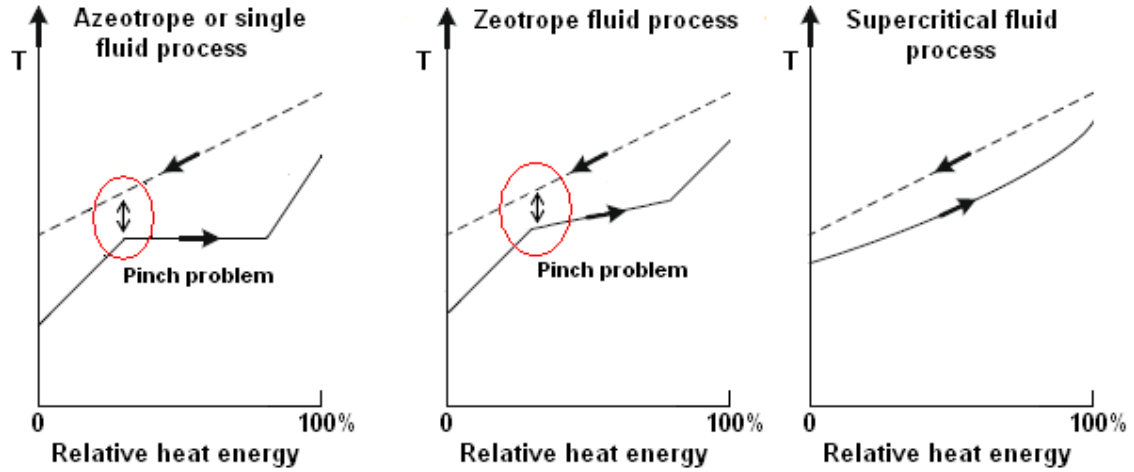
Azeotrope or single fluid process
T
Pinch problem
0
100%
Relative heat energy
Zeotrope fluid process
T
Pinch problem
0
100%
Relative heat energy
Supercritical fluid process
T
0
100%
Relative heat energy

Fig. 1.

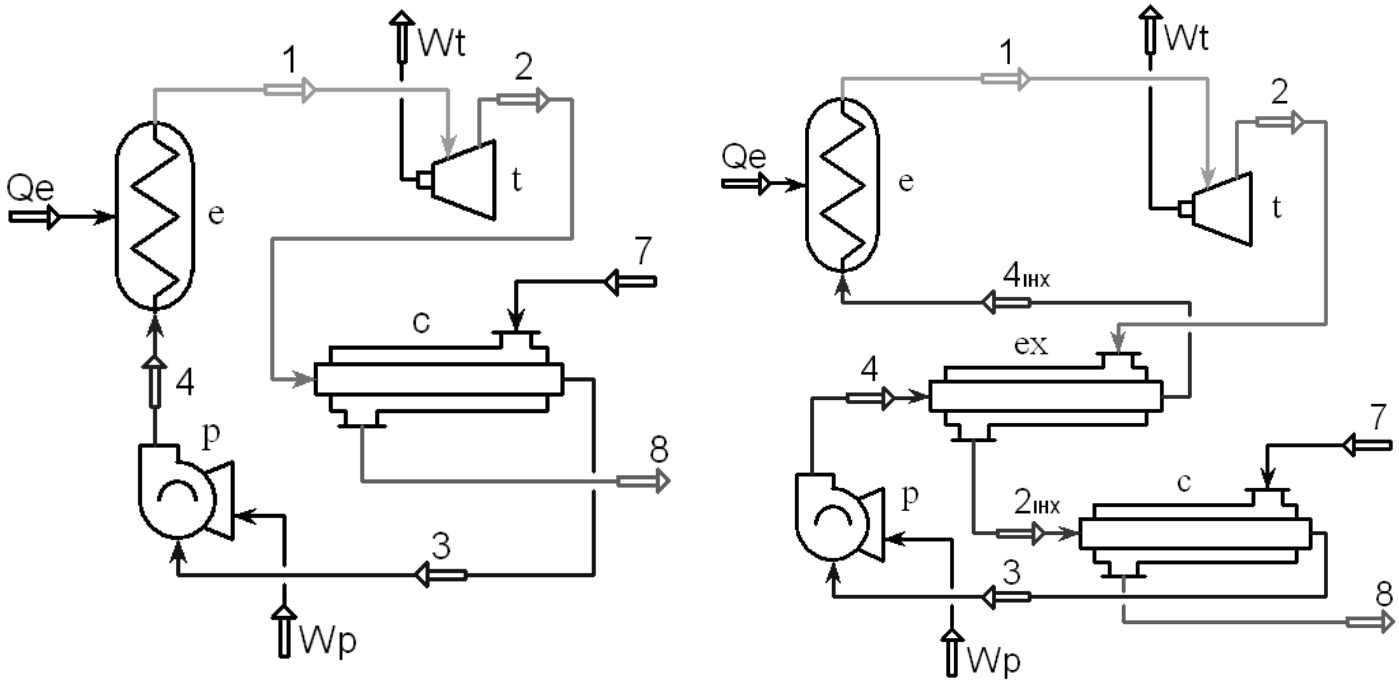
Wt
1
2
Qe
e
t
7
c
4
p
8
3
Wp
Wt
1
2
Qe
e
t
4IHX
ex
4
7
p
2IHX
c
3
8
Wp

a. **b.**

Fig. 2.

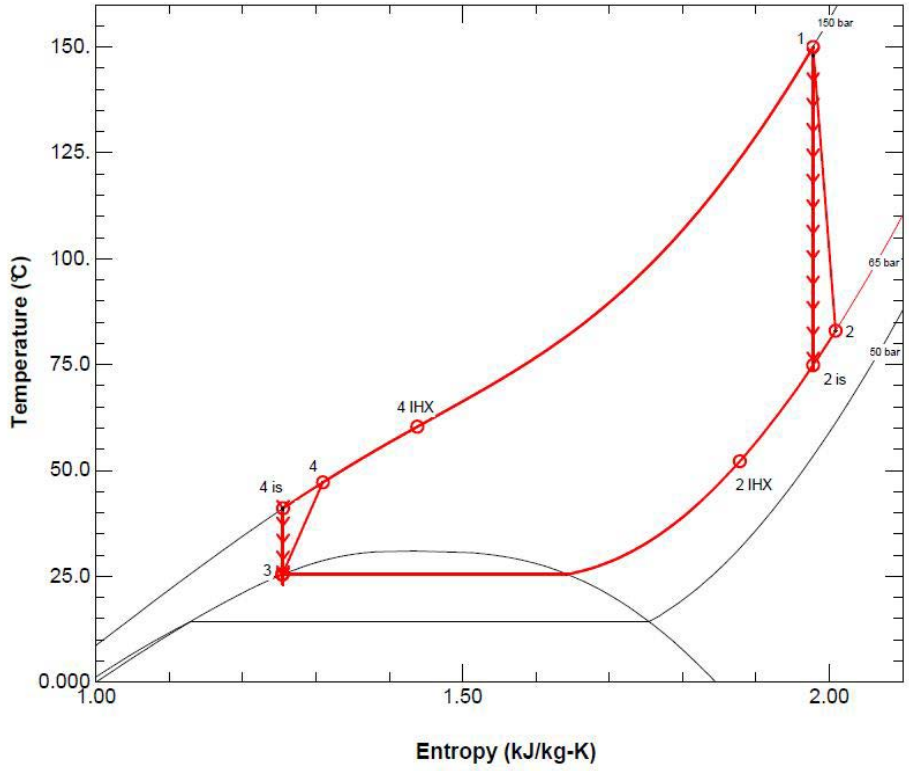
Temperature (°C)
150.
125.
100.
75.0
50.0
25.0
0.000
1.00
1.50
2.00
Entropy (kJ/kg-K)
150 bar
65 bar
50 bar
1
2
2 is
2 IHX
4 IHX
4
4 is
3

Fig. 3.

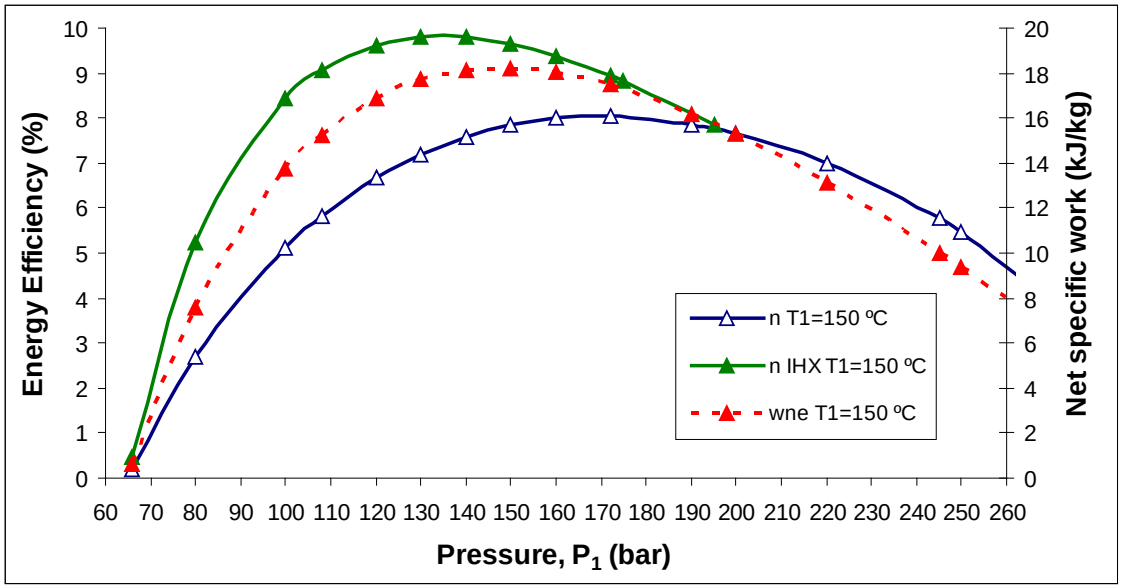
Energy Efficiency (%)
Net specific work (kJ/kg)
Pressure, P1 (bar)
n T1=150 °C
n IHX T1=150 °C
wne T1=150 °C

Fig. 4.

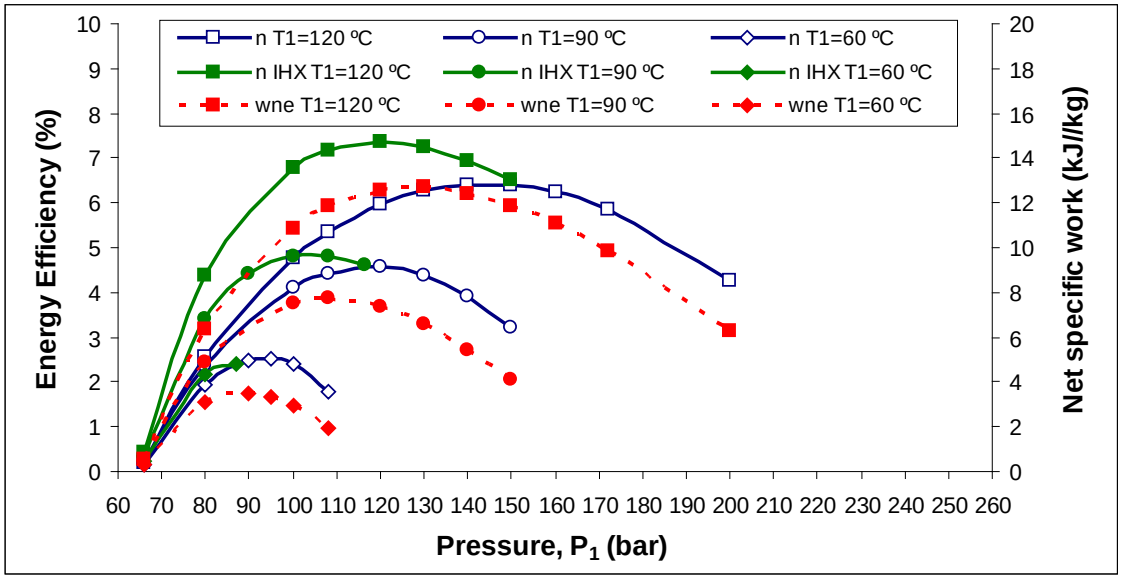
n T1=120 ºC
n T1=90 ºC
n T1=60 ºC
n IHX T1=120 ºC
n IHX T1=90 ºC
n IHX T1=60 ºC
wne T1=120 ºC
wne T1=90 ºC
wne T1=60 ºC
Energy Efficiency (%)
Net specific work (kJ//kg)
Pressure, P1 (bar)

Fig. 5.

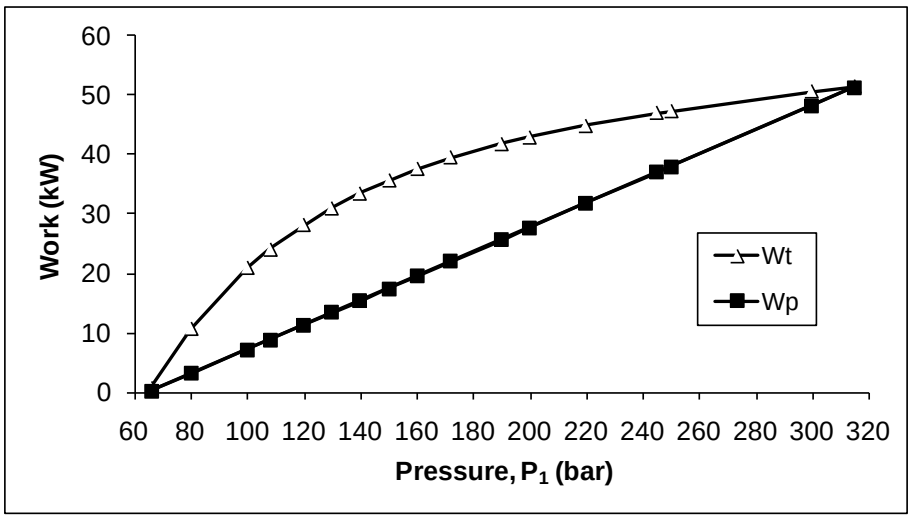
Work (kW)
Wt
Wp
Pressure, P1 (bar)

Fig. 6.

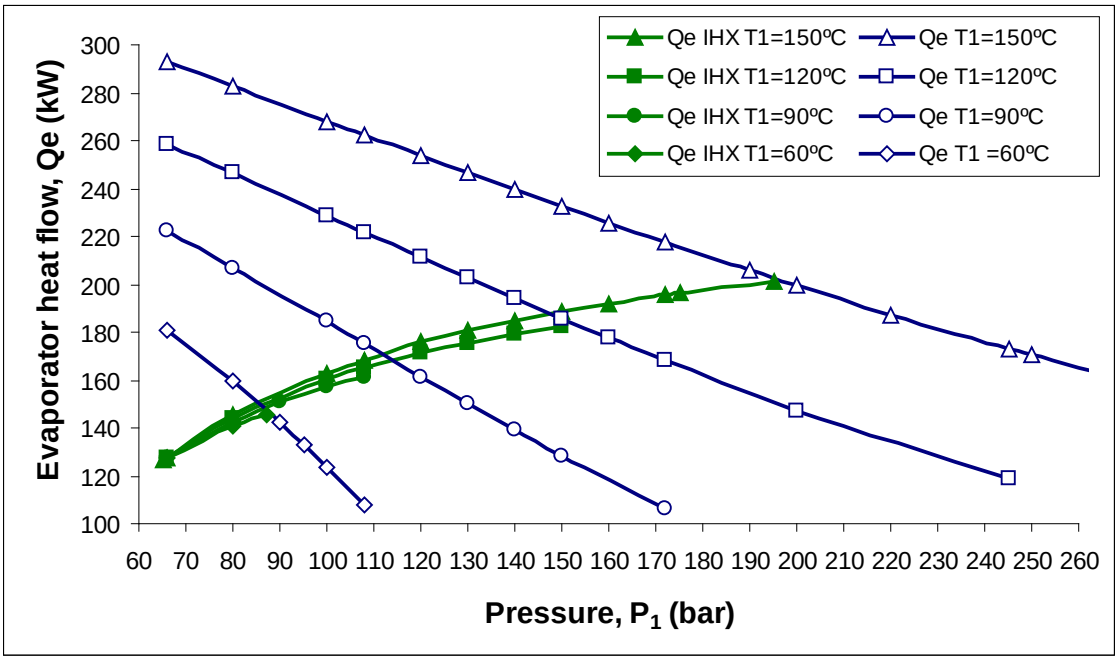
Qe IHX T1=150ºC
Qe T1=150ºC
Qe IHX T1=120ºC
Qe T1=120ºC
Qe IHX T1=90ºC
Qe T1=90ºC
Qe IHX T1=60ºC
Qe T1 =60ºC
Evaporator heat flow, Qe (kW)
300
280
260
240
220
200
180
160
140
120
100
60 70 80 90 100 110 120 130 140 150 160 170 180 190 200 210 220 230 240 250 260
Pressure, P1 (bar)

Fig. 7.

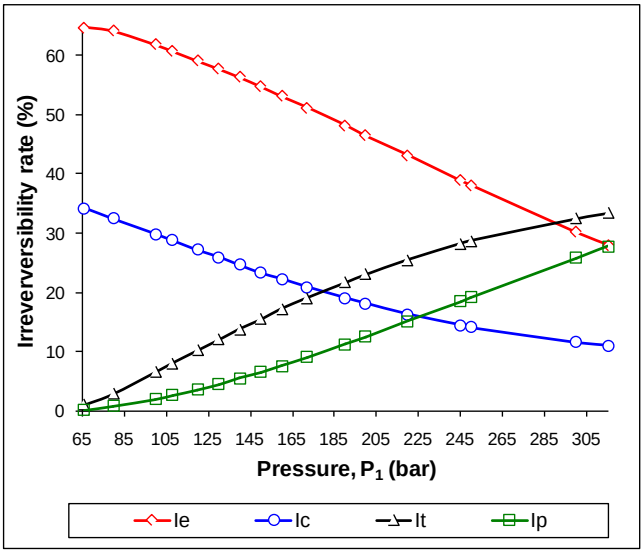
Irreversibility rate (%)
60
50
40
30
20
10
0
65 85 105 125 145 165 185 205 225 245 265 285 305
Pressure, P1 (bar)
Ie
Ic
It
Ip

(a)

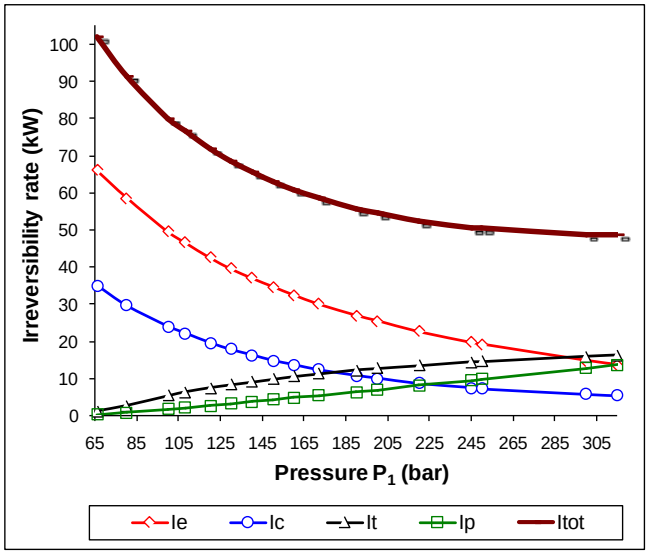
Irreversibility rate (kW)
100
90
80
70
60
50
40
30
20
10
0
65 85 105 125 145 165 185 205 225 245 265 285 305
Pressure P1 (bar)
Ie
Ic
It
Ip
Itot

(b)

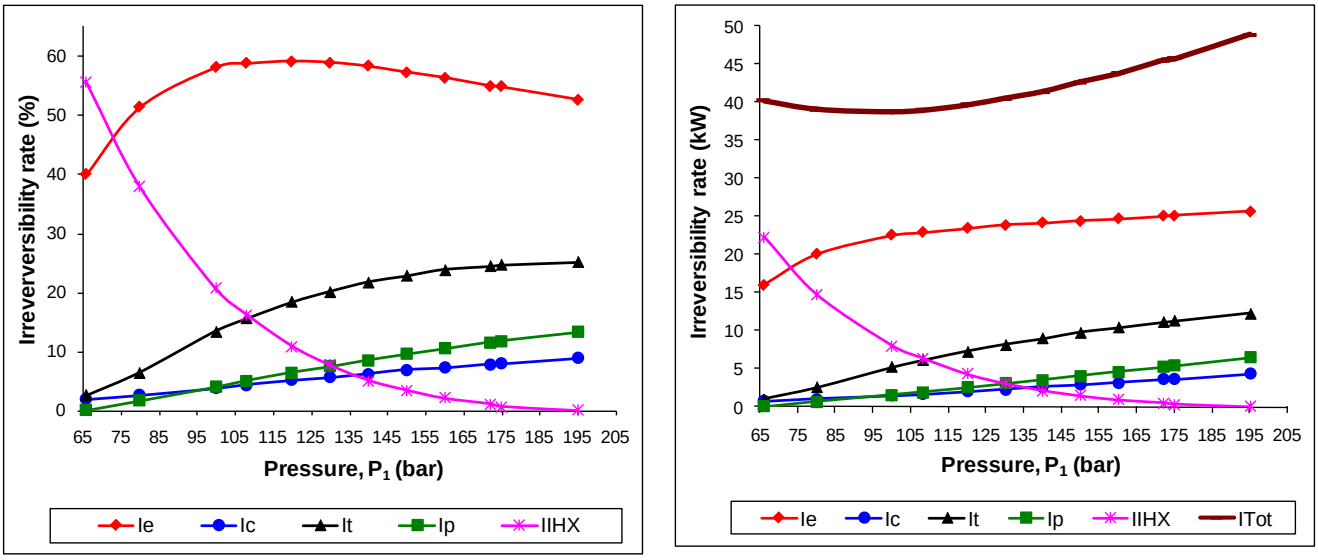
Irreversibility rate (%)
Pressure, P1 (bar)
Ie
Ic
It
Ip
IIHX
Irreversibility rate (kW)
Pressure, P1 (bar)
Ie
Ic
It
Ip
IIHX
ITot

(c) **(d)**

Fig. 8.

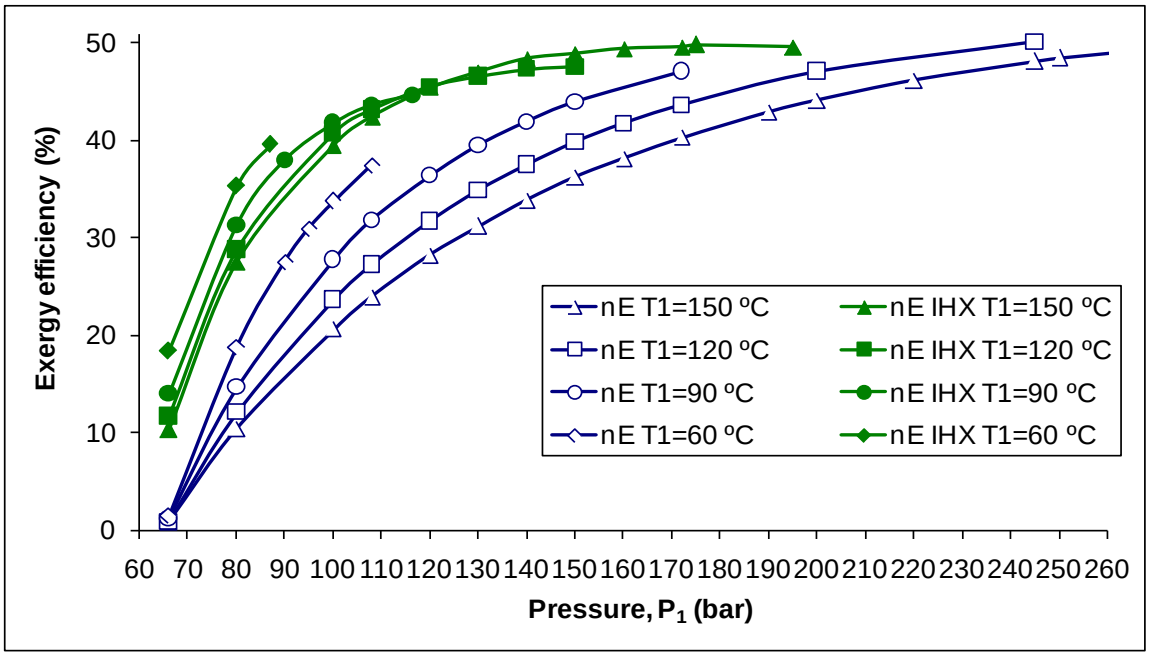
Exergy efficiency (%)
Pressure, P1 (bar)
nE T1=150 ºC
nE IHX T1=150 ºC
nE T1=120 ºC
nE IHX T1=120 ºC
nE T1=90 ºC
nE IHX T1=90 ºC
nE T1=60 ºC
nE IHX T1=60 ºC

Fig. 9.